Macromolecules

ARTICLE

pubs.acs.org/Macromolecules

A Molecular Dynamics Investigation on Mechanical Properties of Cross-Linked Polymer Networks

Nima Nouri and Saeed Ziaei-Rad*

Department of Mechanical Engineering, Isfahan University of Technology, Isfahan 84156-83111, Iran

Ⓢ *Supporting Information*

ABSTRACT: The mechanical properties of Epon-862 cross-linked with curing agent DETDA were simulated using a molecular dynamics code named GPIUTMD fully developed on multi graphical processing units. A new algorithm was proposed to simulate the cross-linking process during the chemical interaction of epoxy with the curing agent without changing the bond data. The models were created by densely packing preconstructed oligomers of different composition and compact them into the periodic simulation box. The properties of interest predicted by the molecular dynamics method were density, glass transition temperature and bulk modulus and found to be in good agreement with available data in the literature. Also, a study on the optimal ratio of resin to cure agent was carried out, and the results showed that, with a 3.6 mix mass ratio, the composite is in its strongest mechanical and structural state.

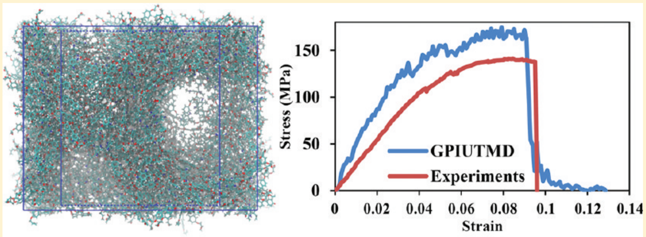

The snapshot of the MD simulation ran with GPUs, system after fracture; and the resulting stress-strain diagram of simple tension in regards to experimental data available.

■ INTRODUCTION

There is a great amount of interest in the development of epoxy resin matrices for use in the composites industry. The modern industries have particular interest in using the epoxy resin Bisphenol-F-diglycidylether (Epon-862 or DGEBF) with the curing agent diethyltoluenediamine (EPI-CURE-W or DETDA) for different applications. Superior mechanical, adhesive, electrical, and chemical resistance properties can be obtained, when Epon-862 is cross-linked with an appropriate curing agent.

Numerical methods of solving the classical equations of motion for multi particle systems with known inter atomic potentials are collectively referred to as molecular dynamics (MD). The MD method was first introduced by Alder and Wainwright in the late 1950s.[1,2] It is nowadays regarded as a major practical application of the classical particle dynamics and has been successfully applied to predict material properties and chemical behavior throughout the past decade.

It is well-known that MD simulation is a technique which needs intensive computation efforts especially in nonbonded pair interactions. Up to now, the system size and the time scale that can be explored using MD are restricted due to the limit in the computational power. For many case studies, one may need to consider several hundred thousands of atoms or a time length from one to thousands of nanosecond. The fast increasing power of the Graphical Processing Units (GPUs) and their streaming architecture opens up a range of new possibilities for a variety of applications. The new GPU chips with their enhanced programability are now capable of performing millions of computation threads simultaneously on a subset of data.

A general purpose MD code fully implemented on the GPU which would be called GPIUTMD hereafter was developed, verified and used for numerical calculations. The goal is to reduce the total computational time of MD simulation with increase in performance/cost ratio without causing any uncertainty in the system response. The implementation was made possible by the use of the NVIDIA CUDA C language API. CUDA provides low level hardware access, avoiding the limitations imposed in fragment shaders. Our hardware consists of three NVIDIA GeForce GTX480 graphic cards.

The early studies on understanding the cross-linking process of polymers were back in the 1980s and 1990s. The main focus of those investigations were basically on the understanding of the reaction kinetics happen in cross-linking process using lattice[3,4] as well as nonlattice[5] methods. As they did not consider the topological information on networks, mechanical and thermodynamic properties of the materials could not be computed. In the late 1990s, several cross-linking approaches using molecular dynamics simulations were proposed for formation of cross-linked network based on topological information.[6,7] It is noteworthy that in the above-mentioned studies, all the cross-linking reactions were assumed to take place simultaneously and in a single step.

Yarovsky and Evans[7] used MD simulation to investigate the strength and molecular mechanisms of adhesion between a cured epoxy resin and an inorganic substrate. The cross-link density in the physical mix of the resin and curing agent molecules was predicted by their technique. However, the reactive sites and covalent bonds formed between the resin and curing agent molecules were not addressed appropriately. Mijovic and Zhang[8] also conducted MD simulation to investigate the interactions and dynamics of water in a fully cured epoxy diethyltoluenediamine

Received: March 13, 2011
Revised: May 10, 2011
Published: June 07, 2011

network. Several molecules of epoxy resin and curing agent were used in MD simulation to describe the cured network material properties.

Gou et al.[9] carried out a combined computational and experimental study of DGEBF−DETDA interacting with single walled carbon nanotubes (SWNT). The cross-linked network of epoxy resins was used to study the interfacial interactions between CNTs and cured epoxy resin in terms of stress transfer. Svaneborg et al.[10] superimposed a stochastic linking procedure on a MD trajectory. By generating cross-linked networks of freely jointed bead−spring chains, they achieved to yield disordered networks consistent with rubbery polymers. Heine et al.[11]used a united atom model to simulate the structural and mechanical properties of large PDMS networks. The simulation was conducted using a dynamic cross-linking approach based on a cutoff distance criterion. The relaxation of the linked structure was carried out through a modified potential. The proposed potential behaved linearly at large distances while at short distances it acted in a quadratic manner. Liang et al.[12] were used molecular dynamics simulations to study the molecular interactions between molecules of (10,10) SWNT and Epon-862 resin and EPI-CURE curing agent W. Their results showed that the aromatic ring structures of both Epon-862/DETDA molecules try to align the aromatic ring planes toward the SWNT surface and wrap around it. They also showed that extension of resin cross-link networks into SWNT cavities can be used to structurally bridge the SWNTs and resin structures to significantly improve the load transfer between them when short SWNTs with openings.

Hamerton et al.[13] created a quasi-crystalline representation for poly cyanurate. This was accomplished by constructing fundamental repeat units at the atomistic scale and chemically joining them in a three-dimensional super lattice. Wu and Xu[14] start from a dense fluid of monomer and linker molecules to develop a model for epoxy. They used a proximity-based cross-link creation algorithm applied progressively throughout an MD trajectory for their model. In a separate study, they also performed cross-linking simulations for epoxy resin and used their model to investigate the diffusion of water in these cross-linked networks.[15] They used an iterative MD/MM procedure to cross-link epoxy resin (DGEBA) where the newly formed topology is subjected to 1000 MD steps of relaxation. This approach carries out one cross-link per iteration, which is bound to have computational limitations when applied to cross-linking of larger systems.

Material properties of Epon-862 cured with TETA curing agent was investigated by Fan et al.[16]using the Accelyrs Simulation package.[17] It should be noted that most of the simulations on formation of cross-linked network have been carried out for quite small model systems. On the basis of varying ratios of cross-linkers to polymer chain ends, Liao et al.[18] were calculated the formation of polymer networks on a coarse-grain level. It is well-known that bulk effective properties of network are function of the degree of cross-linking. Komarov et al.[19] used a four-step reverse mapping procedure using the MC/MD hybrid scheme to capture the physical behavior of highly dense network as a function of cure conversion.

Fully atomistic molecular dynamics simulations were used by Tack and Ford[20] to predict the properties of Epon-862 cross-linked with curing agent DETDA. For this purpose, they used two force fields, namely cff91 and COMPASS. Density, glass transition temperature and bulk modulus were calculated. The results indicate that the COMPASS force field gave more accurate values for the density in compare with experiment. Varshney et al.[21] presented an atomistic model based on molecular modeling for thermosetting polymers. Special emphasis was made on building of atomistic models. Different approaches to build highly cross-linked polymer networks were discussed. A multistep relaxation procedure for relaxing the molecular topology during cross-linking was then proposed. The methodology was then applied to an epoxy-based thermoset (Epon-862/DETDA). Several material properties such as density, glass transition temperature, thermal expansion coefficient, and volume shrinkage during curing were calculated and found to be in good agreement with experimental results.

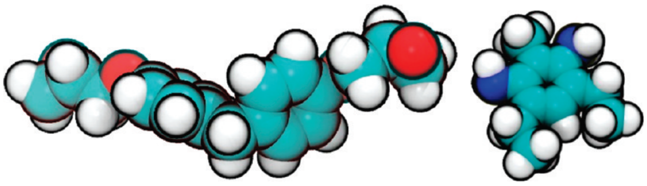

Figure 1. Graphical representation of (a) Epon-862 and (b) DETDA molecular structures.

In this paper, a methodology was developed that requires no change in the bond data nor control over the cross-linking process during the chemical interaction of epoxy with the curing agent. Next, the mechanical properties of Epon-862 cross-linked with curing agent DETDA were simulated using a MD code fully developed on multigraphical processing units. The results are then compared with the available experimental data in literature.

THE MOLECULAR DYNAMICS MODEL

The initial model consists of un-cross-linked epoxy resin Epon-862 and cross-linking agent EPI-Cure-W. The graphical representation of molecular structures, Epon-862 and DETDA are shown in Figure 1. The shape of the model is optimized using the FIRE energy minimization algorithm. It is a coordinate optimization by using a fast inertial relaxation engine.[22]

The average dimension of Epon-862 molecules is around 16.20 Å × 6.67 Å × 4.31 Å, while the size of the DETDA molecules is around 8.31 Å × 5.84 Å × 2.5 Å. According to the experimental data, the mass ratio of Epon-862 to DETDA in the initial mixture was assumed to be 3.5:1. A code which was developed in MATLAB environment gets as input the number of Epon-862 and DETDA molecules and then set up their initial locations randomly in a predefined cell. All the simulations were performed using GPIUTMD molecular dynamics software developed and optimized for running on GPU clusters. The force field used in the calculations is harmonic-bond, harmonic angles and four-body harmonics (harmonic dihedral and improper dihedral). The nonbonded van der Waals interactions were modeled using LJ 12-6 potential. A modified LJ 12-6 potential function was used to model nonbonded interactions between the epoxy and the agent, chain end carbon, and nitrogen atoms, respectively. The initial system was equilibrated using NPT (constant number of atoms, pressure, and temperature) simulations at 400 K and atmospheric pressure for a period of 1 ns. The Nose-Hoover thermostat and Anderson barostat were used for temperature and pressure control, respectively. Periodic boundary conditions were employed in all directions for all simulations in order to reduce and possibly remove the surface effects present in the model. Once the system was equilibrated, the cross-linking was performed as discussed below.

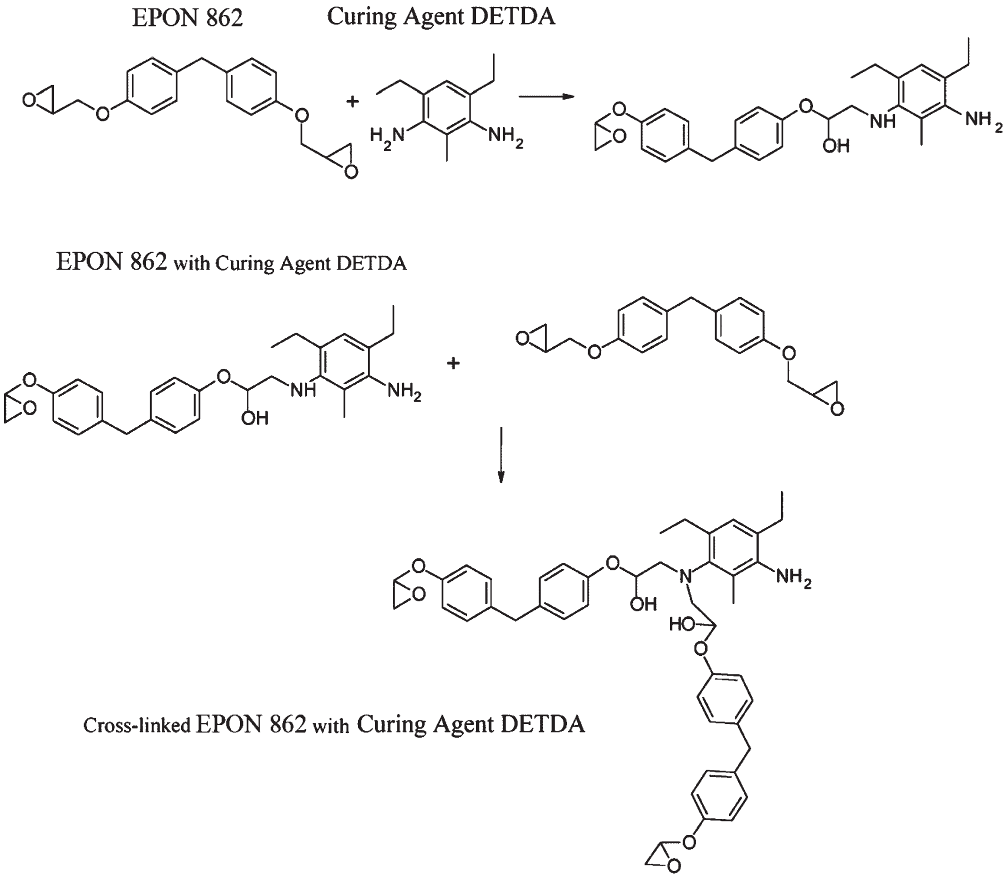

Figure 2. Cross-linking mechanism of Epon-862 at its ends with DETDA curing agent (each cure agent could cross-link with four different Epon-862 before saturation).

The cross-linking between epoxy and agent molecules will start by first hydrating epoxy oxygen atoms at the ends and creating a reactive methylene end group by removing one of its hydrogen atoms. The DETDA's amine group loses both hydrogen atoms to make it chemically active. This was shown schematically in Figure 2. For simulation purpose, it is necessary to adjust the charges on potentially reactive carbon and nitrogen atoms in respective molecules to retain the neutrality of the whole system. The detail description of the procedure used for each single molecule is given in the Supporting Information.

The active nitrogen and carbon atoms that can take part in the process are first tagged by NF and CF respectively. They will be used in a specific potential during the simulations. The LJ potential parameters for the tagged atoms are selected with regard to the following scenario.

1. A single active C atom will fall in the nonbonded well-potential with an active N atom which has not cross-linked yet.
2. The potential parameters are then selected in a manner that it resembles a harmonic potential. In other words, it will not allow an easy separation of the atoms after falling into the well.
3. After the second active C atom trapped into the well, no other active C atom can fall into the well-potential. The repulsive force between active C—C atoms in the case for the third active C is slightly more than the half of the absorbing force between the third active C and N atoms. This will not allow more than two active C atoms to take part in the reaction between epoxy and an agent molecule in each active site or another possibility is that the third atom would replace one of the active C atoms already in cross-link by having enough kinetic energy which has a low probability in room temperature.

The detail of the above scenario is given in the following paragraphs.

The concept of cross-linking between active N and C atoms (i.e., NF and CF) during the chemical interaction of epoxy with the curing agent which is mentioned in steps 1 and 2, is that to replace a harmonic plus an LJ potentials with a single LJ potential with modified parameters. In other words, the difference between the proposed algorithm and existing methods (see for example Varshney et al.[21]) is that in the latter, they used two types of potential for modeling the interaction between active N and C atoms during the chemical interaction of epoxy with the curing agent. For example, when the active N and C atoms are far from each other, the LJ potential is used. However, when the atoms move close to each other so that their distance is about the equilibrium distance (bond length), they switch permanently from LJ to the harmonic potential.

One of the disadvantages of the existing method is that in every step of the simulation the distance between all active C and N atoms should be checked to determine the type of the interaction. This is time-consuming and needs large computational efforts. The other disadvantage of the existing method is that after switching from LJ to harmonic, the separation of active C and N atom is not possible. In our proposed algorithm only one potential is used for

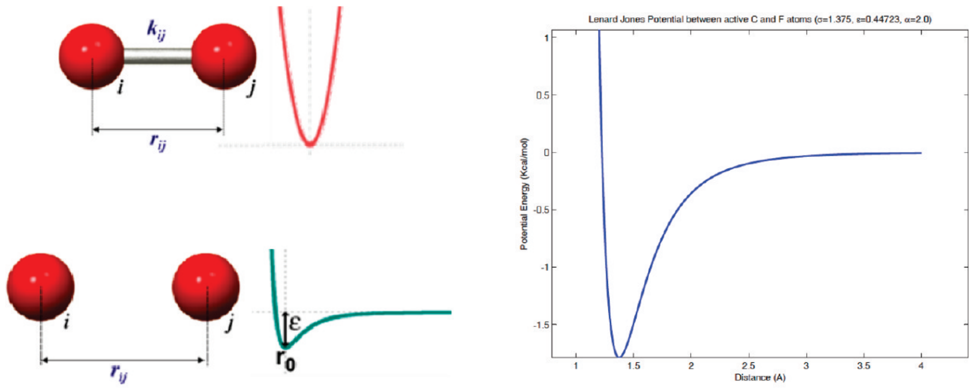

Previous Methods

Presented Method

Figure 3. Comparison between harmonic and standard LJ with modified parameters LJ.

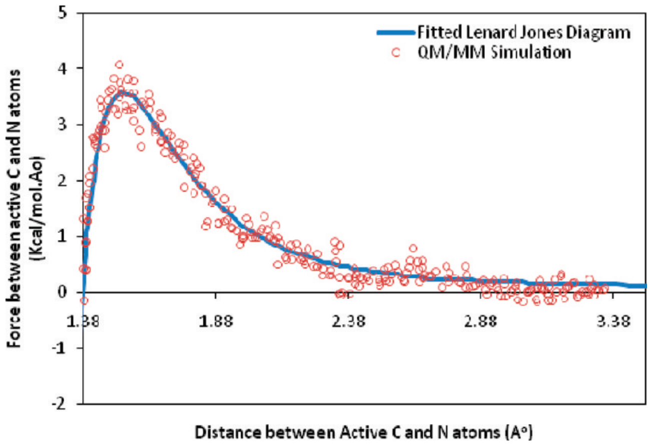

Figure 4. Force−distance diagram for C and N atoms (QM/MM versus fitted LJ).

both of these conditions (before and after bond creation). This was achieved by using an LJ-12-6 potential with proper parameters σ and ε. In other words, we used an LJ with modified parameters instead of a standard LJ plus a harmonic potential (Figure 3). It may result in a minor error in the calculation of interaction force which is negligible with respect to the size of the model. However, the method improves the simplicity of the programming and consequently the calculation speed.

The technique which was used to calculate σ, ε, and α parameters is based on the QM/MM. This was done by the following steps:

- One epoxy and one DETDA molecules were considered. The QM/MM was used to find the equilibrium positions of each atom.
- The distance and the force between one active C and one active N atom are monitored during the simulation.
- An LJ 12-6 force diagram was then assumed and its parameter was determined using least-squares method. Figure 4 shows the data obtained from QM/MM together with the fitted LJ 12-6.
- This procedure was repeated for active N−N atoms.
- The interaction between active C−C was calculated according to the procedure explained below.

The concept of limiting the number of cross-links between active N and C atoms during the chemical interaction of epoxy with the curing agent (i.e., step 3) is implemented automatically into the nonbonded interactions between active C−C atoms.

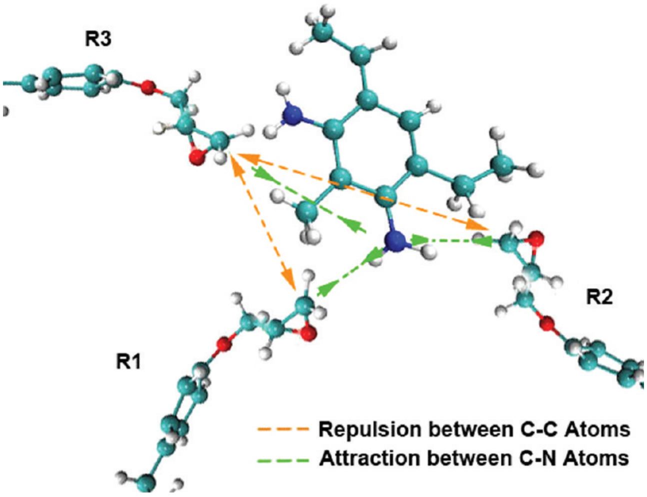

Figure 5. Schematic of cross-linking between active C−C atoms.

The existing methods count the number of reacted cross-links between active N and C atoms. If the saturation limit is reached (2 bonds for active N atom and 1 bond for active C), no new cross-linking will be allowed. In the presented methodology, suppose that two C atoms are interacting with an N atom. Now, assume a third C atom is approaching to the saturated N atom. The distraction force between two C atoms with this new one is more than the attraction between the new C and N atom. This was implemented in the program by choosing a suitable sigma and epsilon for LJ interaction between active C and C atoms. This is schematically shown in Figure 5.

The estimated parameters of LJ equation for active N−N, C−N, and C−C interactions are tabulated in Table 1. The cutoff distance for LJ potential was considered to be 12 Å throughout the model. It is noteworthy that the reaction between active C and N atoms with other atoms are considered as in conventional manner.

Once the cross-linking is completed, there are no left over active C atoms for filling the remaining active sites on unreacted amine nitrogen atoms. The occurrence of this situation can be

Table 1. Non-Bonded Interaction Parameters of CF and NF Atoms

pair	σ	ε	α^*
NF−NF	3.500	0.500 00	2.00
CF−NF	1.375	0.447 23	2.00
CF−CF	3.200	0.400 00	2.00

* α is the parameter used in LJ equations: $4\varepsilon[(\sigma)/(r)^{12} - \alpha(\sigma/r)^6$

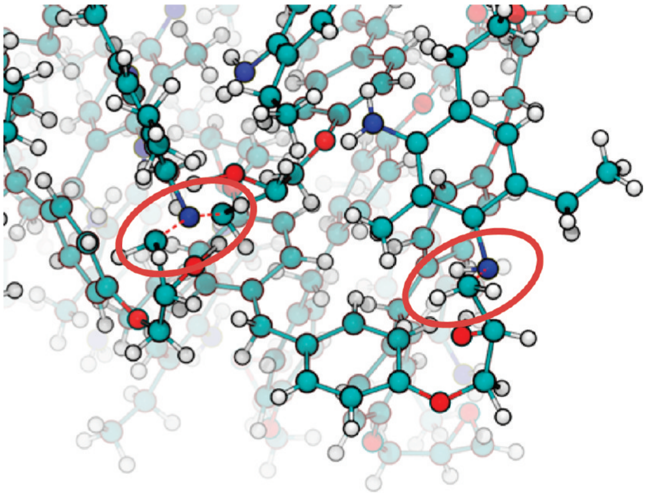

Figure 6. Bonds between epoxy and diethyltoluenediamine active site ends (real footage of simulation steps).

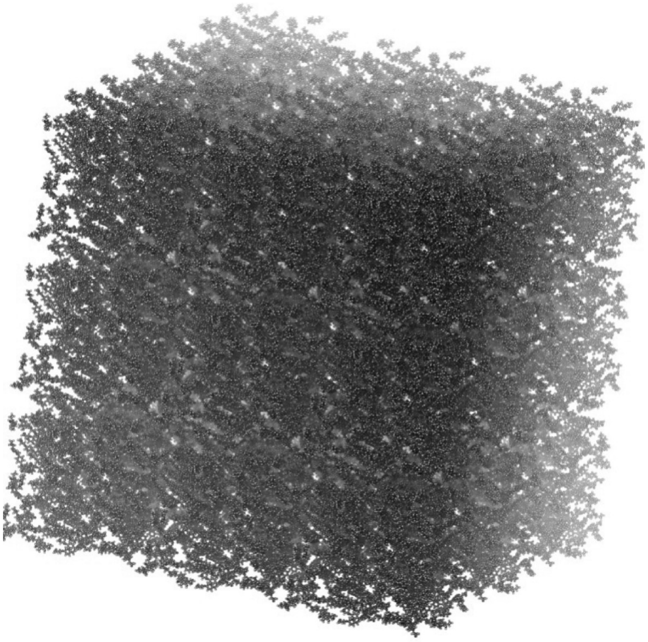

Figure 7. Model of Epon-862 and DETDA agent molecules.

Table 2. Comparison of Various Cross-Linking Approaches

type of energy	un-cross-linked system	cross-linked system
bond energy (per unit)	398 (0.44)	443 (0.48)
angle energy (per unit)	87 (0.06)	163 (0.1)
dihedral energy (per unit)	117 (0.06)	426 (0.18)
van der Waals energy	580	758
Columbic energy	−333	−339
total energy	252	457

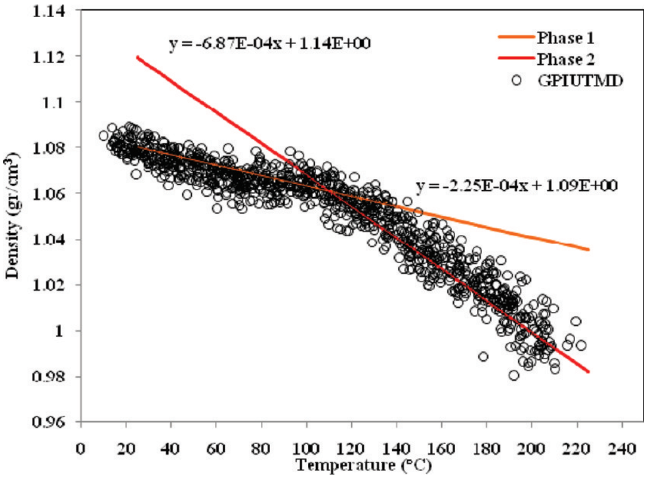

Figure 8. Density of the resin epoxy and cure agent compound versus temperature.

checked by monitoring the amount of nonbonded energy during the solution phase. As already mentioned, the initial locations of molecules inside the model were selected randomly by a developed MATLAB program. The temperature of 400 K, which is the curing temperature for the real condition, allow the molecules to have their long-range movements and find out their minimum locations easily. The system was then cooled down slowly allowing the molecules to reach their minimum energy level. The nonbond potential between active N and C atoms (NF and CF) are shown with dashed lines in Figure 6. Both single cross-linking and double cross-linking are visible in this figure.

The whole model consists of 1700 Epon-862 molecules and 486 DETDA agents. The overall computational size of the system is around 270 000 DOFs. Figure 7 shows the initial random cell of polymer and agent molecules constructed in MATLAB.

From the energy values that listed in Table 2 for un-crossed and cross-linked cases, one can conclude that by increasing the cross-links between molecules, all energies except Columbic energy increases. Xu et al.[14] have also reported such an increase in energetic components upon cross-linking based on Dreiding force field. The increase in bond, angle, and dihedral energies can also be attributed to the newly formed topology. The proposed cross-linking approach leads to a better equilibrated structure as seen by the lowest values of the energetic components. This dynamic cross-linking approach also has another advantage which is its relatively shorter computational time. Also, the presented technique does not require any algorithm to control the cross-linking or saturation process as it is essentially implemented in the formulation.

Figure 8 depicts the density of the cured epoxy versus temperature. Each circle in the graph is a representative for a system state at a specific temperature and density during simulation. The simulation was carried out for several system initial

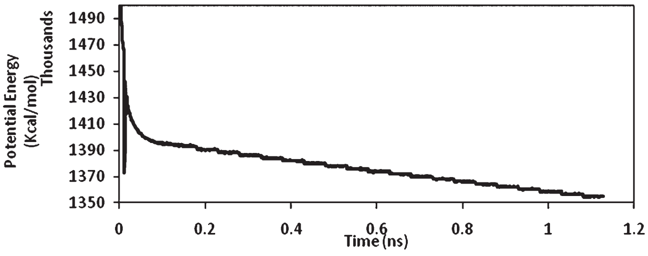

Figure 9. Variation of system potential energy versus time.

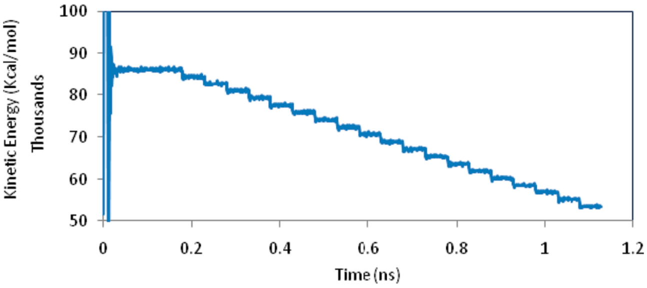

Figure 10. Variation of system kinetic energy versus time.

configurations and it was observed that the average results were similar. The idea was to make sure that the results are independent of the system initial configurations. The figure shows that by decreasing the temperature, the density of the cured epoxy will increase steadily.

A clear change in the slope of the curve is also observable. The change in the slope of the curve is known as the glass transition temperature of the compound. Actually, at this temperature, the resin passes from a glassy state to a rubbery state.

The MD simulation results indicated that the cooling rate can affect the determination of the glass transition temperature. In fact, both temperature and time could be given to the system to allow the molecules to find their minima. In simulations, enough time is given to the system to reach its minimum energy state and this is verified by monitoring both the kinetic and potential energy of the system. Figures 9 and 10 show the variation of the potential and kinetic energy versus time for one of the simulations. In all simulations, the temperature was first set to 400 K and it was observed that after 0.2 ns the graph of potential and kinetic energies of the system reached to a constant value. This means that the equilibrium state of the system was achieved. Then, the temperature was decreased 10 °C and the procedure was repeated. For the next 20 steps, an approximate time of 50 ps was found to be enough for system to reach its stable state.

It is known that the cooling rate can affect the results. In both real situation and in simulation, reducing the cooling rate results in a better curing. This is due to the fact that the molecules have more time to reach their minimum. However, as the simulation costs are very high for simulating with real cooling rate and time, it is a common practice in MD simulation to select a cooling rate for which obtained MD simulation results are in good agreement with the experimental data.[16,21] Therefore, by tuning this parameter it was found that a value of 10 °C/50 ps will give a glass temperature (T_g) close to the experiments.[23] It is noteworthy to mention that using a cooling rate less than 10 °C/50 ps will not change the calculated glass temperature.

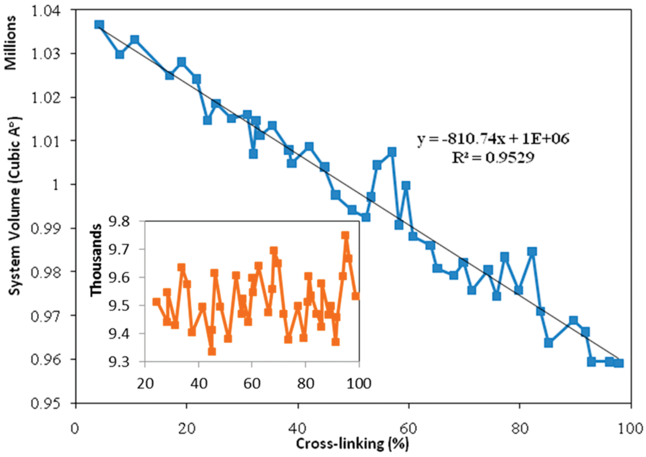

Figure 11. Volume shrinkage as a function of percent of cross-linking (the red graph is the volume change for a small model that consists of 28 Epon-862 and eight curing agent molecules).

Table 3. MD Simulation and Experimental Data for the Resin Epoxy and Cure Agent Compound

parameter	MD simulation	experimental data[23]	error %
T_g	107.52	105	2.40
β (*below* T_g)	56.23	61.0	7.82
β (*below* T_g)	196.2	195.0	1.26
modulus of elasticity	3.52	3.43	2.62

For epoxy-based systems, the volume shrinkage or increase in the density is observed experimentally during the process of network formation. In order to observe this shrinkage, the instantaneous volume of the system during the relaxation stage of cross-linking simulations was tracked continuously and plotted in Figure 11. The results are indicating that by increasing the percentage of cure conversion, an increase in density is observable. This is in agreement with the results reported recently by Kamorov.[19] Figure 11 also shows that the volume of the system decreases by increasing the number of cross-linked change. This decrease was about 7.55%. This is comparable to the shrinkage results observed by Yarovski[7] where the authors observe volume shrinkage of 5−12% for different systems. It is also important to note here that such a volume shrinkage could not convincingly observed for system with small number of molecules mainly because of significant statistical variations in the results (Figure 11). This is shown in the orange graph plotted in Figure 11. To plot the orange graph, a system consists of 28 Epon-862 and 8 curing agent molecules were considered. Because of statistical variations in the results which are considerable in small systems, the change in the shrinkage of the system does not show any specific trend.

Table 3 compares the glass transition temperature obtained from the MD simulation with that of the experiment. The table also contains two other parameters, namely linear thermal expansion coefficient and the modulus of elasticity of the compound.

For isotropic materials, the linear thermal expansion coefficient, β, is related to the volumetric thermal expansion coefficient by the following formula:

$$\beta = \frac{1}{3}\alpha \tag{1}$$

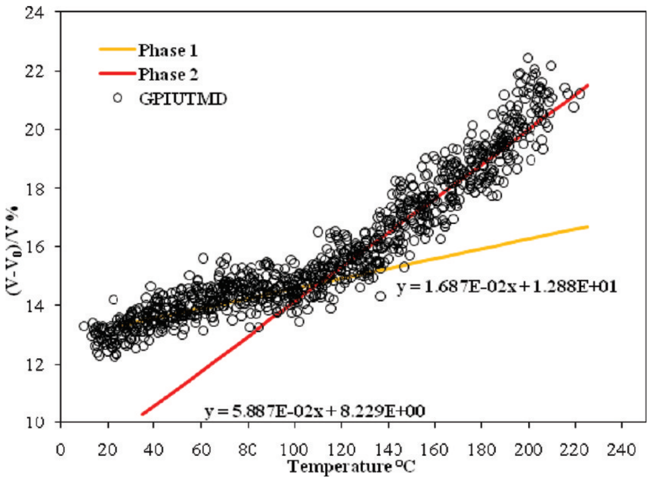

Figure 12. Volume changes versus temperature for resin epoxy and cure agent compound.

The volume thermal expansion coefficient, α, is defined using the following equation

$$\alpha = \frac{1}{V}\left(\frac{\partial V}{\partial T}\right)_P \qquad (2)$$

where T is the temperature, P is the pressure, and V is the volume. Therefore, by calculating the volume of the system at each temperature step, while pressure is kept constant (*NPT* ensemble), one can calculate the volumetric thermal expansion coefficient

$$\alpha = \frac{1}{V_i}\left(\frac{V_i - V_0}{\Delta T}\right)_P \qquad (3)$$

where V_0 is the initial volume of the system and V_i are the volume of the system at T_i.

Figure 12 depicts the graph of $(V - V_0)/V$ versus temperature. Two lines are then fitted to the calculated data, one line to the data before the transition glass temperature and another to the data after T_g. The results were then used to calculate the linear expansion coefficients which are tabulated in Table 3. In the presented method, the percentage of the cross-linking after curing was around 95%. It means that most of the molecules were reacted with each other and created a network of macromolecules.

Other important factors that can be extracted from the simulations are geometrical characteristics of the system. One of these parameters is the system fractal dimension. Once MD has been used to generate the samples, the fractal dimension can be calculated based on the pair distribution function (PDF) of the samples. The PDF represents the probability of finding a pair of atoms separated by a distance r in the structure, relative to the probability expected for a randomly distributed structure having the same density.[24] The PDF is calculated as

$$\begin{aligned} g_{\alpha\beta}(r_1, r_2) &= \frac{V^2}{N_\alpha N_\beta}\left\langle \sum_{i=\{\alpha\}}^{N_\alpha} \sum_{j=\{\beta\}}^{N_\beta} \delta(r_1 - r_i)\delta(r_2 - r_j)\right\rangle \\ &= \rho_\alpha^{-1}\rho_\beta^{-1}\left\langle \sum_{i=\{\alpha\}}^{N_\alpha} \sum_{j=\{\beta\}}^{N_\beta} \delta(r_1 - r_i)\delta(r_2 - r_j)\right\rangle \qquad (4) \end{aligned}$$

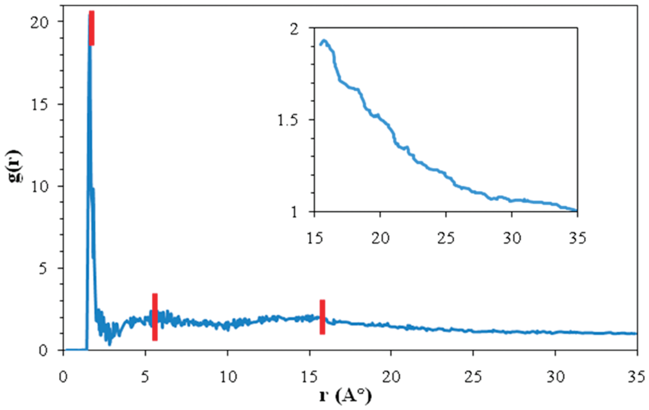

Figure 13. Pair distribution function of CF and NF atoms versus distance.

where V is the volume of the system, N_α and N_β are the number of particles of entities of type α and β respectively, ρ_α and ρ_β are the corresponding densities of α and β subsystems, and the symbol $\langle\rangle$ means ensemble average. Therefore, several configurations of the system should be used to compute the PDF. The term inside the $\langle\rangle$ symbol indicates that when finding the distribution of distances between the atoms of type α and β, one must locate each atom of type α and obtain the distance from it to all atoms of type β. An example of the PDF for one of the systems created in this study is shown in Figure 13. The figure indicates the decay of the PDF for large values of the distance between the atoms (i.e., r). The decay can be used to estimate the fractal dimension, d_f, of the systems by using the relation:[25]

$$d_f = 3 + \frac{\mathrm{d}[\log(g(r))]}{\mathrm{d}[\log(r)]} \qquad (5)$$

The fractal dimension is a geometrical parameter which shows how good the molecules fill the space. The fractal dimension of 3 for example in this case means a bulk epoxy/DETDA composite without any voids or free spaces. The main idea of this analysis was to check the results of simulation with the reported experimental data and show that the geometry of the system is similar to the real one. The fractal dimension of the system was found to be 2.17 ± 0.02 which is close to the experimental data of 2.21 reported by Chu and Wu.[26] There are three distinct peaks observed in the pair distribution function (PDF) of CF and NF atoms in Figure 13. The first peak which is the largest pick is located at $r = 1.375$ Å while the second and third extremes are in 5.30 and 16 Å, respectively. These are related to nonbonded neutral length, distance between two active sites in a DETDA agent and distance of active ends of epoxy resins, respectively. This diagram benchmarks the idea of the cross-linking and resin chains production by using the modified nonbonded potential pairs. The peaks are more apparent in large models as the probabilistic uncertainties are less effective in such models.

The mechanical properties were determined during the simulation by calculating the virial stress and monitoring the cell dimensions and then plotting the results. The method for calculation of virial stresses are presented as Supporting Information. As already mentioned we have used LJ with modified parameters to express the interaction between NF and CF atoms. By increasing the strain on the system, the nonbonded (LJ) interactions between molecules are weakened and allow

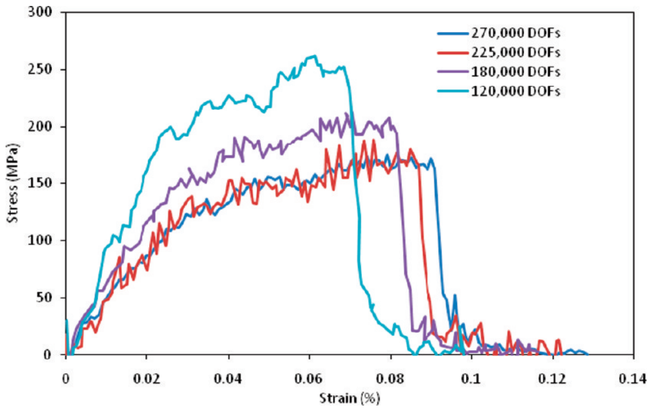

Figure 14. Stress−strain curve for system with different DOFs (convergence study).

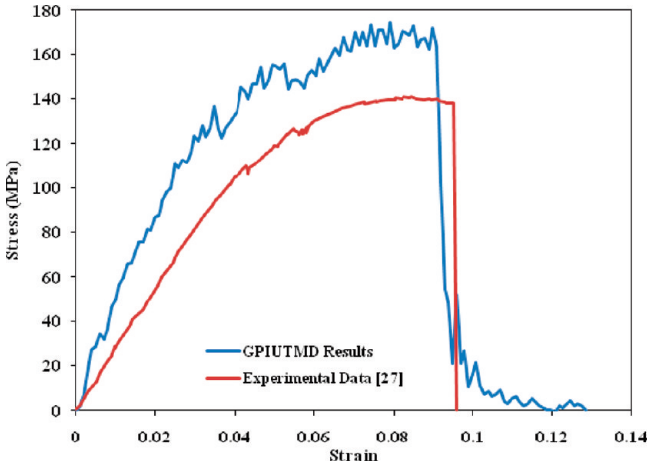

Figure 15. Stress−strain diagram of epoxy/cure agent composite (1550 Epoxy molecules and 730 DETDA).

separation of molecules and eventually lead to the system failure. Also, many models with different number of atoms were tested. A convergence study was carried out to find out the adequate number of atoms for a converged simulation. The diagram presented in the paper is the converged diagram. For the sake of clarity the results are reported for four simulations with 40, 60, 75, 90 thousands atoms in Figure 14.

The final stress strain diagram obtained from the simulation of tension test is shown in Figure 15. From mechanical point of view, the slope of the first 0.3% strain can be used to calculate the Young modulus of the composite. However, Figure 15, which is plotted for the whole range of strain, shows the relative good agreement between the predicted and experimental data.[27] The difference may be due to the fact that all bond forces in our simulation are assumed linear.

The simulation results follow the experimental test data with about maximum 17% error, which is reasonable. As it is clear from the figure, the experimental and MD results are coincide until 0.3% strain and this is why the MD model can predict the Young's modulus almost accurately. The difference between the numerical and measured stress for strains larger than 0.3% can be reduced by considering more accurate force fields such as Morse, Yukawa, and Gauss instead of harmonic potentials which may predict the nonlinear behavior of the material in large deformations in a more appropriate way. The simulation also shows a fracture in the material for a strain of 9%. The calculated ultimate tensile strength for the material is 170 MPa which is around 30 MPa higher than that of the real material.

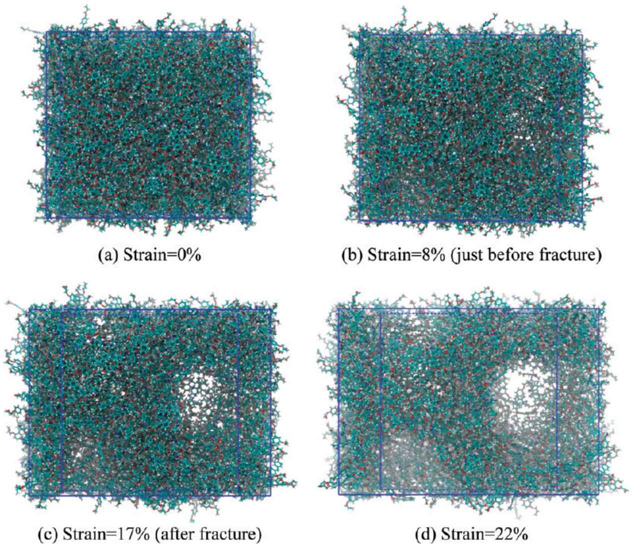
(a) Strain=0%
(b) Strain=8% (just before fracture)
(c) Strain=17% (after fracture)
(d) Strain=22%

Figure 16. The snapshot of the system at different strain rates (1550 Epoxy molecules and 730 DETDA).

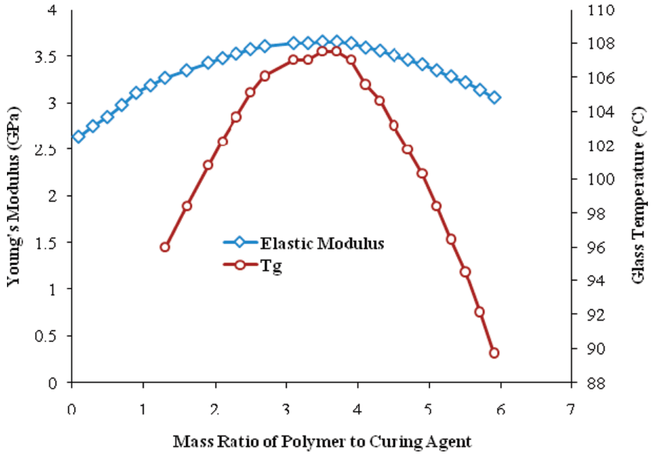

Figure 17. Variation of Young's modulus and glass transition temperature versus mass ratio of polymer to curing agent.

Figure 16 shows a snapshot of a small system just after the fracture. At about a strain of 8%, the void nucleation starts emerging all over the structure which confirms the fact that the material is isotropic. Voids became very large and the structure will be tearing off at a high strain value. Parts c and d of Figure 16 depict the void nucleation and its growth inside the model.

The simulation steps described before is used to find the behavior of the material, namely elastic modulus and glass transition temperature, in different mass ratios of polymers to curing agents. The results depicted in Figure 17 show an optimal mass mixing ratio of about 3.6, which is near to the values proposed in standard texts for manufacturing of this composite. Both properties reach their maximum values at this optimum point. This can be explained by the fact that, for a well-cured system, there are more activated cross-links which results in a stronger structure.

By keeping the number of resin molecules constant and increasing the cure agents, i.e., decreasing the mass ratio of polymer to curing agent, the surplus of the cure agents will reduce the integrity of the structure which in turn decreases the system mechanical performances. For such a case, the MD simulations also predicted the agglomeration of compounds in several locations inside the simulation box. However, on the other hand, when insufficient cure agents exist in the model, there are more empty active sites for cross-linking, which results in an unsaturated and weak structure.

CONCLUSIONS

In this study, elastic properties of Epon-862/DETDA composite were numerically investigated using a general MD code fully developed on GPUs. The classical molecular dynamics simulation with the well-verified Dreiding potential was employed. A specific Lennard-Jones potential was proposed which correctly models the curing process of the system without changing the model bonds. The model consists of great numbers of resin and the curing agent. The results have demonstrated the usefulness of the MD simulations as a tool to determine the material characteristics of cross-linked epoxy resin and curing agent compound.

The predicted material properties from MD simulations are in good agreement with the experimental values from the literature, which confirms the accuracy of the cured epoxy resin model, and the properness of the force field.

The change of the elastic modulus and also glass temperature versus the mass ratio of the composite was observed. The calculated modulus of elasticity was about 3.5 GPa at the optimal mass ratio of 3.6. The presented technique could also properly predict the fracture point of the material. The approach was also able to find out the mechanical behavior of the system in an appropriate amount of time.

ASSOCIATED CONTENT

Ⓢ **Supporting Information.** Description of the charge update strategy, force field parameters and virial stress. This material is available free of charge via the Internet at http://pubs.acs.org.

AUTHOR INFORMATION

Corresponding Author

*Telephone: +98 311 391 5244. Fax: +98 311 391 2628. E-mail: szrad@cc.ut.ac.ir.

REFERENCES

(1) Alder, B. J.; Wainwright, T. E. *J. Chem. Phys.* **1957**, *27*, 1208.

(2) Alder, B. J.; Wainwright, T. E. *J. Chem. Phys.* **1959**, *31*, 459.

(3) Rohr, D. F.; Klein, M. T. *Ind. Eng. Chem. Res.* **1990**, *29*, 1210.

(4) Schulz, M.; Frisch, H. L. *J. Chem. Phys.* **1994**, *101*, 10008.

(5) Eichinger, B. E.; Shy, L. Y.; Leung, Y. K. *Macromolecules* **1985**, *18*, 983.

(6) Doherty, D. C.; Holmes, B. N.; Leung, P.; Ross, R. B. *Comput. Theor. Polym. Sci.* **1998**, *8*, 169.

(7) Yarovsky, I.; Evans, E. *Polymer* **2002**, *43*, 963.

(8) Mijovie, J.; Zhang, H. *J . Phys. Chem. B* **2004**, *108*, 2557.

(9) Gou, J. H.; Minaie, B.; Wang, B.; Liang, Z. Y.; Zhang, C. *Comput. Mater. Sci.* **2004**, *31*, 225.

(10) Svaneborg, C.; Grest, G. S.; Everaers, R. *Polymer* **2004**, *46*, 4283.

(11) Heine, D. R.; Grest, G. S.; Lorenz, C. D.; Tsige, M.; Stevens, M. J. *Macromolecules* **2004**, *37*, 3857.

(12) Liang, Z.; Gou, J.; Zhang, C.; Wang, B.; Kramer, L. *Mater. Sci. Eng., A* **2004**, *365*, 228.

(13) Hamerton, I.; Howlin, B. J.; Klewpatinond, P.; Shortley, H. J.; Takeda, S. *Polymer* **2006**, *47*, 690.

(14) Wu, C. F.; Xu, W. J. *Polymer* **2006**, *47*, 6004.

(15) Wu, C. F.; Xu, W. J. *Polymer* **2007**, *48*, 5440.

(16) Fan, H. B.; Yuen, M. M. F. *Polymer* **2007**, *48*, 2174.

(17) Accelrys Inc.: San Diego, CA.

(18) Yang, W.; Wei, D.; Jin, X.; Liao, Q. *Macromol. Theory Simul.* **2007**, *16*, 548.

(19) Komarov, P. V.; Yu-Tsung, C.; Shih-Ming, C.; Khalatur, P. G.; Peineker, P. *Macromolecules* **2007**, *40*, 8104.

(20) Tack, J. L.; Ford, D. M. *J. Mol. Graph. Model.* **2008**, *26*, 1269.

(21) Varshney, V.; Patnaik, S.; Roy, A. K.; Farmer, B. L. *Macromolecules* **2008**, *41*, 6837.

(22) Bitzek, E. *Phys. Rev. Let.* **2006**, *97*, 170201.

(23) Morris, J. E. In *Nanopackaging: nanotechnologies and electronics packaging*; Springer: Portland, OR; 2008, 49, 50.

(24) Allen, M. P.; Tildesley, D. J., *Computer Simulation of Liquids*; Oxford University Press: New York, 1994.

(25) Kieffer, J.; Angell, C. A. *J. Non-Cryst. Solids* **1988**, *106*, 336.

(26) Chu, B.; Wu, Ch. *Macromolecules* **1988**, *21* (6), 1729.

(27) Watson, T. http://tiims.tamu.edu/2005summerREU/papers/Watson.pdf, 2007.